FUSE

Fungal Systematics and Evolution

VOLUME 10
DECEMBER 2022
PAGES 127–137

doi.org/10.3114/fuse.2022.10.05

Globisporangium coniferarum sp. nov., associated with conifers and *Quercus* spp.

F. Salmaninezhad[1], F. Aloi[2], A. Pane[2], R. Mostowfizadeh-Ghalamfarsa[1]*, S.O. Cacciola[2]*

[1]Department of Plant Protection, School of Agriculture, Shiraz University, Shiraz, Iran 7144167186 1
[2]Department of Agriculture, Food and Environment (Di3A), University of Catania, Catania, Italy 95123

*Corresponding authors: rmostofi@shirazu.ac.ir, olga.cacciola@unict.it

Key words:
Conifers
Globisporangium
new taxon
oomycete
phylogenetic analyses
Pythiaceae

Abstract: During a survey of gardens in Shiraz County, Iran, aimed at identifying oomycetes associated with roots of ornamental trees, a species of *Globisporangium* with distinctive morphological characters separating it from other known species in this genus was recovered from conifers and occasionally from a *Quercus* sp. Five isolates of this species were characterised. Phylogenetic analyses of nuclear (ITS and *βtub*) and mitochondrial (*cox1* and *cox2*) loci using Bayesian inference and maximum likelihood analyses as well as their distinct morphological and cultural characteristics (*e.g.,* abundant production of chlamydospores; globose, ellipsoid to ovoid sporangia; amorphous oogonia with a smooth wall; paragynous to rarely hypogynous antheridia and 1–5 antheridia per oogonium; mostly plerotic oospores) revealed that these isolates belong to a new *Globisporangium* species grouping in the phylogenetic clade G of *Pythium sensu lato*. This paper formally describes *Globisporangium coniferarum sp. nov*. as a new species and compares it with other phylogenetically related and already known *Globisporangium* species, including *G. nagaii*, *G. violae*, *G. paddicum, G. okanoganense, G. iwayamae* and *G. canariense*.

Citation: Salmaninezhad F, Aloi F, Pane A, Mostowfizadeh-Ghalamfarsa R, Cacciola SO (2022). *Globisporangium coniferarum sp. nov*., associated with conifers and *Quercus* spp. *Fungal Systematics and Evolution* **10**: 127–137. doi: 10.3114/fuse.2022.10.05
Received: 22 July 2022; **Accepted:** 7 September 2022; **Effectively published online:** 26 October 2022
Corresponding editor: P.W. Crous

INTRODUCTION

Green spaces are of great significance for the quality of urban life (Nowak *et al.* 2005). Persian gardens have a long tradition and inspire the design of many historical gardens in other parts of the world, from the Alhambra in Spain to the Taj Mahal and Humayun's tomb in India. Shiraz, the capital of Fars province (Iran), is famous for its gardens, such as the Eram Garden, a historical Persian landscape garden that was declared a World Heritage site. Numerous oomycetes have been reported to be associated with the roots and rhizosphere of landscape trees. *Phytophthora* species have been reported to cause root rot and decline of trees, including conifers, in gardens, parks and nature reserve areas worldwide (Erwin & Ribeiro 1996, Barber *et al.* 2013, Jung *et al.* 2019, Giordana *et al.* 2020, Khdiar *et al.* 2020, Riolo *et al.* 2020, La Spada *et al.* 2022). Several oomycetes have been reported from conifers in Iran, including *P. nicotianae* (from *Cupressus arizonica* and *Pinus pinaster*), *P. citrophthora* (from *Pinus sylvestris* and *Pinus elderica*), *P. cactorum* (from *Pinus nigra*), *P. citricola* (from *Pinus taeda*), and *Pythium* sp. (from *Pinus sylvestris*) (Mirabolfathy & Ershad 1993, Mirabolfathy & Ershad 1996, Ershad 2009).

The genus *Pythium* was previously divided into 11 phylogenetic clades (A–K) based on DNA sequence data of the ITS region. Clades E, F, G, I and J produced globose to ovoid sporangia (Lévesque & de Cock 2004). Members of clade K were allocated in a new genus, *Phytopythium* (de Cock *et al*. 2015). Uzuhashi *et al.* (2010) confirmed the findings of previous molecular studies, indicating *Pythium* to be a paraphyletic genus, and divided it into five phylogenetic clades (1–5) using phylogenetic data of the 28S rDNA and *cox2* gene regions. Clade 4, the largest clade, was described as a new genus, *Globisporangium*, encompassing clades E–G, I and J *sensu* Lévesque & de Cock (2004). According to Uzuhashi *et al.* (2010) species of *Globisporangium* produce globose, internally proliferating sporangia, although other shapes of sporangia may also sporadically occur in this genus. Based on both phylogeny and morphology, Uzuhashi *et al.* (2010) emended *Pythium sensu stricto* (*s.s.*) encompassing clades A–D *sensu* Lévesque & de Cock (2004), and, along with *Globisporangium*, segregated from *Pythium sensu lato* (*s.l.*) three other new genera, *Ovatisporangium* (phylogenetic clade K, syn. *Phytopythium*), *Elongisporangium* (clade H) and *Pilasporangium*, the last not coinciding with any of the 11 clades introduced by Lévesque & de Cock (2004). Very recently, the split of *Pythium s.l.* into several genera was confirmed and consolidated using a phylogenomic approach, and the generic names introduced by Uzuhashi *et al.* (2010) were accepted, with the only exception of *Ovatisporangium*, which was shown to be a later synonym of *Phytopythium* (Nguyen *et al.* 2022). There are only a few reports of *Globisporangium* species from Iran, among which *G. nunn* (from *Zea mais, Oryza sativa* and *Robidia hispida*) and *G. debaryanum* (from *Oryza sativa*) (Bolboli & Mostowfizadeh-Ghalamfarsa 2015, Salmaninezhad & Mostowfizadeh-Ghalamfarsa 2017, 2019a). Moreover, some species of *Pythium* reported from Iran phylogenetically group within the genus *Globisporangium* and have been renamed accordingly by Nguyen *et al.* (2022); they

include *G. ershadii* (formerly, *P. ershadii*, typus from uncultivated soil), *G. iranense* (formerly *P. iranense*, typus from soil under *Prunus armeniaca*), *G. kandovanense* (formerly *P. kandovanense*, typus from leaves of *Lolium perenne*), *G. monoclinum* (formerly *P. monoclinum*, typus from uncultivated soil), *G. pyrioosporum* (formerly *P. pyrioosporum*, typus from soil under *Capsicum annuum*), and *G. urmianum* (formerly *P. urmianum*, typus from soil under *P. dulcis*).

Globisporangium has a worldwide distribution and species of this genus, including among others *G. splendens* and *G, ultimum*, have been reported on conifers (Lazreg *et al.* 2013, Uzuhashi *et al.* 2019). Moreover, several species of *Pythium s.l.,* including *P. intermedium*, *P. irregulare* and *P. ultimum* were reported to be responsible for damping-off of coniferous seedlings in numerous countries. After the taxonomic revisions of Uzuhashi *et al.* (2010) and Nguyen *et al*. (2022), these three species were included in the genus *Globisporangium* and renamed *G. intermedium*, *G. irregulare* and *G. ultimum*, respectively (Darvas *et al.* 1978, Elvira-Recuenco *et al.* 2020). However, there are no reports of *Globisporangium* species on conifers in Iran.

The present paper describes a new species of *Globisporangium* isolated from conifers and occasionally from a *Quercus* sp. during a survey of gardens in Shiraz County, Iran, aimed at identifying oomycetes associated to roots of declining ornamental trees. This new species shows unique morphological features and has also been distinguished based on multi-locus phylogenetic analysis.

MATERIALS AND METHODS

Isolation

Samples were randomly collected from rhizosphere soil of ornamental trees showing symptoms of decline in Shiraz gardens, Fars Province, during 2017 to 2019. The trees had brown to black crowns and generally showed decline symptoms such as wilting, defoliation, and dieback, as well as root and crown rot. The disease affected *Pinus elderica* trees more than other hosts. Coordinates were recorded for each sampling site by Global Positioning System (GPS) (Table 1). Samples were transported to the Mycology Laboratory of the Department of Plant Protection, Shiraz University. One hundred grams of each soil sample were placed in a plastic container and flooded with tap water to 1 cm above the soil surface (Tan 1996). Isolates were recovered from samples by baiting with 5 mm surface sterilized bitter orange (*Citrus aurantium*) leaf disks or 5 mm pieces of sterile meadow grass (*Poa annua*) at 25 °C every 8 h for 40 h in total, and plating on CMA-PARP (cornmeal agar, ground corn extract 40 g/L; agar 15 g/L; amended with 10 µg/mL pimaricin, 200 µg/mL ampicillin, 10 µg/mL rifampicin and 25 µg/mL PCNB) (Jeffers & Martin 1986). Isolates were purified via hyphal tips on water agar (WA, Agar 10 g/L) and stored on CMA (extract of 40 g/L ground corn; agar 15 g/L) slopes at 15 °C. Stock cultures were maintained on CMA slopes at 15 °C in the dark.

Morphological characterisation

In order to observe asexual organs (sporangia, vesicles and zoospores), isolates were transferred to CMA containing sterile hemp (*Cannabis sativa*) seeds or turfgrass (*Poa* sp.) leaves (Mostowfizadeh-Ghalamfarsa & Banihashemi 2005) for 24 h. Hemp seeds or turfgrass were then transferred to Petri dishes containing distilled water (Ho *et al.* 2012), sterile soil extract (McLeod *et al.* 2009) or Schmitthenner solution (Schmitthenner 1973) under fluorescent light for 48 h and were checked every 8 h for six times. Sporangia formation was also examined using French bean agar medium (FBA, extract of 30 g/L French bean; agar 15 g/L) (Jeffers & Martin 1986) and sterile soil extract (Mostowfizadeh-Ghalamfarsa *et al.* 2008). Sexual organs were obtained with hemp seed agar (HSA, ground hemp seed extract 60 g/L; agar 15 g/L) and carrot agar (CA, carrot extract 250 g/L; agar 15 g/L) incubated in darkness. To study colony morphology, isolates were grown on CMA, HSA, CA, potato-dextrose agar

Table 1. List of *Globisporangium coniferarum* isolates recovered from conifers and *Quercus* sp. in Shiraz County, Iran, with their corresponding CBS and GenBank accession numbers.

Isolate codes[1]	Date of collection	Location	Longitude	Latitude	Matrix	GenBank accession number			
						ITS	*βtub*[a]	*cox1*[b]	*cox2*[c]
GbCu04-2* = CBS 148568	Jul. 2018	Shiraz; Golestan BLVD	29.620.813	52.562.442	*Cupressus arizonica* (Root tissue)	ON554847	MZ020764	MZ020754	MZ020759
ChQu06 = CBS 148564	Jun. 2018	Shiraz; Chamran BLVD	29.663.553	52.487.497	*Quercus* sp. (Crown tissue)	ON554845	MZ020767	MZ020757	MZ020762
ErCu18 = CBS 148565	Sep. 2018	Shiraz; Eram Garden	29.635.622	52.525.659	*Cupressus sempervirens* (Soil)	ON554846	MZ020766	MZ020756	MZ020761
MgPi02 = CBS 148566	Aug. 2018	Shiraz; Mahmoudieh BLVD	29.670.653	52.490.953	*Pinus elderica* (Crown tissue)	ON554844	MZ020763	MZ020753	MZ020758
ErLa03 = CBS 148567	Aug. 2018	Shiraz; Eram BLVD	29.635.622	52.525.657	*Cupressus sempervirens* (Soil)	ON554843	MZ020765	MZ020755	MZ020760

[1] Abbreviations of isolates and culture collections: CBS = Westerdijk Fungal Biodiversity Institute, Utrecht, The Netherlands; other isolate names and numbers are as given by the collectors. * ex-holotype species.

[a] β-tubulin. [b] cytochrome c oxidase subunit I; [c] cytochrome c oxidase subunit II.

Table 2. Morphological and morphometrical (µm) features of *Globisporangium coniferarum* isolates from conifers and *Quercus* sp. in Shiraz County, Iran.

Isolates	Sporangium			Main hypha			Oogonium			Oospore			Antheridium		
	Average	Range	Shape	Average	Range	Shape	Average	Range	Type	Average	Range	Wall	Shape	Average	Range
GbCu04-2	23.412	12.815–29.701	Mostly globose	3.414 ± 0.5	2.501–6.011	Globose to amorphous	25.432 ± 1.5	17.741–26.911	Aplerotic	19.122 ± 1.5	16.631–26.104	1.111 ± 0.5	Clavate	5.311	4.324–6.211
ChQu06	23.534	15.548–30.005	Mostly globose	3.124 ± 1.0	2.555–5.841	Globose to amorphous	25.392 ± 1.1	18.003–27.843	Aplerotic	20.003 ± 1.2	17.238–26.004	1.512 ± 1.1	Clavate	5.234	4.031–6.004
ErCu18	25.005	20.013–30.342	Mostly globose	3.659 ± 1.3	3.005–6.124	Globose to amorphous	26.362 ± 0.5	17.751–26.555	Aplerotic	19.321 ± 0.5	16.385–25.474	1.323 ± 1.0	Clavate	5.405	4.127–6.124
MgPi02	24.301	19.984–30.012	Mostly globose	3.103 ± 1.1	2.381–5.003	Globose to amorphous	25.471± 1.2	17.304–26.711	Aplerotic	19.113 ± 2.5	16.112–26.120	1.396 ± 1.5	Clavate	6.004	4.983–6.549
ErLa03	23.013	16.873–27.564	Mostly globose	3.013 ± 1.5	2.444–6.013	Globose to amorphous	26.001 ± 1.0	18.683–27.904	Aplerotic	20.43 ± 0.7	17.005–26.492	1.123 ± 0.7	Clavate	5.125	4.005–6.139

(PDA, potato extract 300 g/L; dextrose 20 g/L; agar 15 g/L) and malt extract agar (MEA, 25 g/L; agar 15 g/L) (Mostowfizadeh-Ghalamfarsa & Banihashemi 2005). Plugs (5 mm diam) from the edge of a 3-d-old culture were placed on Petri dishes, each containing 20 mL of a test medium (*i.e.*, CMA, HSA, CA, MEA, and PDA). The plates were incubated at 25 °C for 48 h. Temperature-growth relationships were tested on PDA with three replicate plates per isolate and incubated at 0, 5, 10, 15, 20, 25, 30, 35 and 40 °C. Growth rate was recorded 2–12 d after the onset of linear growth.

DNA extraction, PCR, sequencing and phylogenetic analyses

The method described by Mirsoleimani & Mostowfizadeh-Ghalamfarsa (2013) was employed for DNA extraction. Potato extract broth (extract of 300 g/L boiled potato in distilled water) was used for growth of isolates. Mycelium was harvested, freeze dried, and DNA extract was obtained using the DNG™-PLUS extraction kit (CinnaGen, Teheran, Iran) according to the manufacturer's instruction. DNA quality was examined with an MD-1000 NanoDrop machine (NanoDrop Technologies, Wilmington, DE, USA). The primers used for amplification and sequencing of nuclear (internal transcribed spacers 1, 2 and 5.8S gene of rDNA = ITS and β-tubulin gene = *βtub*) as well as mitochondrial (cytochrome c oxidase subunit I = *cox1* and cytochrome c oxidase subunit II = *cox2*) loci are listed in Table S1. The PCR conditions for these loci are listed in Table S2. PCR products were detected in 1 % agarose gel and purified products were sequenced by Macrogen Europe (Amsterdam, The Netherlands). The sequence quality of the ITS region using ITS4 and ITS6 region was quite low and this region was consequently cloned to obtain clear sequences. The ITS amplification of the primer pairs DC6 and LR0 (Tables S3, S4) were diluted by a factor of 10 and cloned into *Escherichia coli* using the StrataClone PCR cloning kit (Agilent Technologies, USA) following the manufacturer's instructions. Single colonies were transferred into 20 µL of distilled molecular biology grade water and PCR conducted with Mango DNA polymerase (Bioline, UK). Reaction mixes of 12.5 µL contained 1× Mango Reaction buffer, 200 µM dNTPs, 2 mM $MgCl_2$, 0.8 µg BSA (bovine serum albumin, Carl Roth GmbH, Germany), 0.4 µM of M13 forward (5'- GTAAAACGACGGCCAG- 3') and M13 reverse (5'- CAGGAAACAGCTATGAC -3') plasmid primers, 0.5 U of Mango DNA Polymerase and 0.5 µL of the colony suspension as a template. PCR was carried out on an Eppendorf Mastercycler pro S system equipped with a vapo.protect lid with an initial denaturation at 96 °C for 10 min, 36 cycles at 96 °C for 20 s, 54 °C for 20 s and 72 °C for 60 s, concluding with a final elongation at 72 °C for 4 min. Positive clones were sent for sequencing to the laboratory centre of the Senckenberg Biodiversity and Climate Research Centre (BiK-F, Frankfurt, Germany) using the plasmid primer T3 (5'- ATTAACCCTCACTAAAGGGA) and T7 (5'- TAATACGACTCACTATAGGG) as well as DC6 and LR0. Sequence data were deposited into GenBank.

Resulting sequences were edited by BioEdit (Hall 1999). Sequence alignment was performed using ClustalX (Thompson *et al.* 1997) with subsequent visual adjustment. Partition homogeneity tests were conducted on combined nuclear and mitochondrial gene alignments by PAUP v. 4.0a136 (Swofford 2002) using 100 replicates and heuristic general search option. BLAST similarity searches were performed with blastn (for nucleotide-versus-nucleotide comparison) (Altschul *et al.* 1990). In order to reconstruct the phylogenetic trees, Bayesian inference analyses on individual and concatenated ITS, *βtub , cox1,* and *cox2* loci were carried out with MrBayes v. 3.1 (Ronquist & Huelsenbeck 2003), imposing a general time reversible (GTR) substitution model with gamma (G) and proportion of invariable site (I) parameters to accommodate variable rates across sites. Bayesian analyses were conducted with the same dataset according to Safaiefarahani *et al.* (2015) and Salmaninezhad & Mostowfizadeh-Ghalamfarsa (2019b). The best nucleotide substitution model was determined by MrModelTest v. 2.3 (Nylander 2004). Two independent runs of Markov Chain Monte Carlo (MCMC) using four chains were run over 1 000 000 generations. Trees were saved each 1 000 generations, resulting in 2 002 trees. Burn-in was set at 5 % of the saved trees. To conduct phylogenetic comparisons, maximum likelihood was also used by PHYLIP DNAML (Felsenstein 1993) for the combined tree. The robustness of the maximum likelihood trees was estimated by 1 000 bootstraps. *Elongisporangium anandrum* was chosen as outgroup (Table S3). Phylogenetic trees were edited and displayed with TREEGRAPH (Stöver & Muller 2010). The alignments and trees were submitted to Figshare (https://www.figshare.com; doi: 10.6084/m9.figshare.20893672).

Table 3. Comparison of morphological features of *Globisporangium coniferarum* with closely related species.

Character	*G. coniferarum*	*G. canariense*	*G. nagaii*	*G. paddicum*	*G. okanoganense*	*G. iwayamae*	*G. violae*	*G. monoclinum*
Cardinal Temperatures (°C)	15;30;40	No data	9;28;35	No data	5;20;<30	5;25;30	5;25;35	5;25;35
Daily Growth Rate at 25 °C (mm)	6	14–15	25	No data	4	14	15	14
Colony Pattern on CMA	Radial submerged	Chrysanthemum	No data	No data	Submerged	Submerged, vaguely radiate	With aerial mycelium	Submerged
Hyphae (µm)	3.1–7.3	7	4	No data	8	6.6	6	5
Chlamydospore	(+), (sub)globose, ovoid	-	-	-	-	+	-	-
Sporangium or Hyphal Swelling Production (µm)	(+) 16.3–17.6	(+) 18–30	(+)	(+) 25–30	(+) 30–35	(+) 28–48 × 44	(+) 25–30	(+) 15–26
Sporangium or Hyphal Swelling Shape	Ellipsoid, globose, ovoid, with pedicel	Spherical, (sub) globose, pyriform, peanut-shape, dumb-bell shape, elongated	Ovoid, pyriform	(Sub)globose, oval, limoniform	(Sub)globose to pyriform	Spherical, ellipsoidal, ovoid, papillate	Globose	Globose to occasionally subglobose
Sporangium Proliferation	-	-	+	+	+	-	-	-
Sporangium or Hyphal Swelling Position	Mostly terminal	Mostly intercalary and catenulate	Terminal	Terminal	Terminal	Termianl	Terminal or intercalary	Terminal or intercalary
Zoospore Production	+	+	+	+	+	+	-	-
Homothallic/Heterothallic	Homothallic	Homothallic	Homothallic	Homothallic	Homothallic	Homothallic	Homothallic	Homothallic
Oogonium Ornamentation	Smooth	Smooth	Smooth	Ornamented	Smooth	Smooth	Smooth	Smooth
Oogonium Shape and Dimensions (µm)	Globose, ovoid, ellipsoid, 25.9–26.7	Spherical, 19–30	Globose, sometimes irregular, 14–22	Globose (No data)	Globose, 24–30	Globose (No data)	Globose, 27–38	(Sub)globose, rarely elongated, 16–26
Antheridium Shape	Clavate to no specific shape	Mostly sessile	Clavate	Clavate to sessile	Crook-naked	Clavate	Sessile	Sessile
Antheridium Type and Number per Oogonium	Monoclinous and diclinous, paragynous, rarely hypogynous, 1–5	Monoclinous, paragynous, 1–6	Monoclinous, 1 (disappears after fertilization)	Monoclinous and diclinous, 1–4	Monoclinous and diclinous, 1–3	Monoclinous and diclinous, 1–3	Mostly monoclinous,1-8	Mostly monoclinous, 1–2
Oospore Type and Dimensions (µm)	Aplerotic and plerotic, 21.3–23.2	Plerotic, 17–29	Aplerotic, 12–19	Aplerotic, (No data)	Aplerotic to mostly plerotic, 22–27	Aplerotic and plerotic, 19–24	Aplerotic, 24–30	Plerotic, rarely aplerotic, 10–24
Oospore Wall (µm)	1.9–3.1	2–4	0.8	No data	1.5–3	No data	3	2
Number of Oospore per Oogonium	1	1	1	1	1	1	1	1

RESULTS

During the survey of urban gardens in Shiraz County, various oomycete isolates were sourced, including 500 isolates of *Pythium s.l.* Among 365 isolates of *Globisporangium* spp. recovered from conifers, one distinct group was detected, which was not referable to any known *Globisporangium* species; this group also included an isolate from *Quercus* sp. (Table 1). This group clustered into clade 4, *Globisporangium sensu* Uzuhashi *et al.* (2010), according to phylogenetic trees based on ITS, *ϐtub, cox1,* and *cox2* sequences (Figs S1–S4), each of which showed that this group constituted a well-supported monophyletic lineage. Isolates of this group produced globose to subglobose and pedicellate sporangia as well as detaching vesicles, and smooth-walled oogonia. The oogonia showed diverse shapes, from globose to ovoid or ellipsoid. The combination of morphological characteristics of this group of isolates was unique compared to the other known species of *Globisporangium*.

Phylogenetic analyses

Isolates of this group had identical sequences of both nuclear and mitochondrial genes. The *ϐtub* sequences of the isolates showed 99 % similarity with *G. nagaii* (JX397970)*, G. sylvaticum* (MK752998)*,* and 98 % similarity with *Pythium* sp. (EF195140), and *Phytopythium oedochilum* (DQ071326). The *cox1* sequences of the isolates showed 98 and 99 % similarity with *Pythium* sp. (MG182704) and *G. mamillatum* (GU071819), respectively. The *cox2* sequences had 99 % similarity with *G. nagaii* (JX397984), *G. attrantheridium* (GU071764), and *G. spinosum* (MN381730). Despite our repeated efforts for sequencing, ITS sequences using ITS4 and ITS6 primer pairs as well as DC6 and LR0 primer pairs alone, showed extremely poor quality. To address the problem of low-quality ITS sequences, we conducted cloning of the ITS region. At first, using T3 and T7 universal primer pairs for sequencing did not work well and only the 18S region of ITS rDNA had a good sequencing quality. To address this problem, we performed two main approaches: (1) Performing the colony PCR using M13 forward and reverse primer after allowing the clones to grow for 24 h, and (2) Sequencing of the inserted region in the plasmid using DC6 and LR0 primers. Using these two approaches, we obtained high-quality sequences of the ITS region. The ITS sequences of the isolates showed 88.77 % similarity with *Pythium* sp. MNS2014a (KM047893.1), *Globisporangium* sp. MT2021c (LC644723.1), and 88.47 % similarity with *G. nagaii* (KU211238.1).

The final alignment length was 508 bp for *cox2,* 457 bp for *ϐtub,* 610 bp for *cox1,* 1406 bp for ITS, and 3 011 bp for combined gene regions (Table S4). All trees resulting from Bayesian inference and maximum likelihood analyses showed similar topologies, hence, Bayesian trees were shown with both Bayesian posterior probability and maximum likelihood bootstrap values. The new group of isolates formed a well-supported monophyletic clade in all phylogenetic trees (Bayesian posterior probability 0.89–1.00; maximum likelihood bootstrap support 100 %; Fig. 1). In the *ϐtub* tree, the isolates clustered in the vicinity of *G. nagaii, G. nunn* and *G. perplexum* (Fig. S1). In other trees, the isolates clustered in the proximity of *G. nagaii, G. okanoganense*, *G. violae*, *G. iwayamae*, and *G. paddicum* (Figs S2–S4).

Taxonomy

Globisporangium coniferarum Salmaninezhad & Mostowf., ***sp. nov.*** MycoBank MB 838368.

Etymology: The name refers to the conifers, the host plants from which isolates of this species were recovered most frequently.

Typus: **Iran**, Fars Province, Shiraz (29.620.813, 52.562.442), isolated from the roots of *Cupressus arizonica*, 10 Jul. 2018 (Table 1), *F. Salmaninezhad* (**holotype** CBS 148568 stored in a metabolically inactive state, fungarium of the Westerdijk Fungal Biodiversity Institute, Utrecht, The Netherlands; culture ex-type GbCu04-2 = CBS 148568); GenBank: *ϐtub* = MZ020764; *cox2* = MZ020759; *cox1* = MZ020754; ITS = ON554847.

Colonies on CMA show a chrysanthemum pattern, on PDA and MEA show an intermediate and rosette pattern, respectively, and on HSA show a radial submerged pattern (Fig. 2). Main hyphae have 3.1–7.3 (av. 7) µm width. Abundant chlamydospores formed both in liquid and solid media (*i.e.*, CMA and HSA). *Chlamydospores* are globose, subglobose, and ovoid, terminal and intercalary, and are 17.5–23.8 (av. 23) µm diam (Fig. 3). *Sporangia* are ellipsoid, globose to ovoid, with pedicels, without papillae, non-proliferating, mostly terminal and rarely intercalary, 16.3–17.6 (av. 17) µm diam (Fig. 3). In contrast to the abundant chlamydospore formation, few vesicles and zoospores form after 36–72 h at 25–30 °C. *Vesicle* formation is unique in this taxon, in which the vesicle smoothly separates from the sporangium and discharges in a farther position from the sporangium. Zoospore release does not easily progress in this taxon, and it lasts for at least 20 min. *Oogonia* are globose, ovoid, and ellipsoid, smooth, terminal and intercalary, 25.9–27.6 (av. 27) µm (Fig. 3). *Antheridia* are 1–5 per oogonium, clavate to no specific shape, terminal and intercalary, diclinous and monoclinous, with a terminal contact, paragynous, rarely hypogynous (Fig. 3). Antheridium origination in monoclinous oospores is near oogonium stalk. *Oospores* are globose, mostly plerotic 21.3–23.2 (av. 22.0) µm with a wall which is 1.9–3.1 (av. 3 µm) µm thick. Morphometric results are shown in Table 2. Colonies on PDA have an average radial growth rate of 6 mm at 25 °C. Cardinal temperatures: optimum 30 °C, minimum 15 °C, and maximum 40 °C (Fig. 4). Key characteristics that distinguish *Globisporangium coniferarum* from other closely related species of *Globisporangium* are shown in Table 3.

Additional isolates examined (paratypes , stored as metabolically inactive cultures): **Iran**, Fars Province, Shiraz (29.663.553, 52.487.497), from the crown of *Quercus* sp., 9 Jun. 2018, *F. Salmaninezhad*, *ChQu06* (culture ex-paratype CBS 148564), GenBank: *ϐtub* = MZ020767; *cox2* = MZ020762; *cox1* = MZ020757; ITS = ON554845; Fars Province, Shiraz (29.635.622, 52.525.659), from rhizosphere soil of *Cupressus sempervirens*, 16 Apr. 2018, *F. Salmaninezhad*, *ErCu18* (culture ex-paratype CBS 148565), GenBank: *ϐtub* = MZ020766; *cox2* = MZ020756; *cox1* = MZ020761; ITS = ON554846; Fars Province, Shiraz (29.670.653, 52.490.953), from the crown tissue of *Pinus elderlica*, 12 May 2018, *F. Salmaninezhad, MgPi02* (culture ex-paratype CBS 148566), GenBank: *ϐtub* = MZ020763; *cox2* = MZ020758; *cox1* = MZ020753; ITS = ON554844; Fars Province, Shiraz (29.635.622, 52.525.657), from rhizosphere soil of *Melaleosa citrina*, 15 Jun. 2018, *F. Salmaninezhad, ErLa03* (culture ex-paratype CBS 148567), GenBank: *ϐtub* = MZ020765; *cox2* = MZ020760; *cox1* = MZ020755; ITS = ON554843 (Table 1).

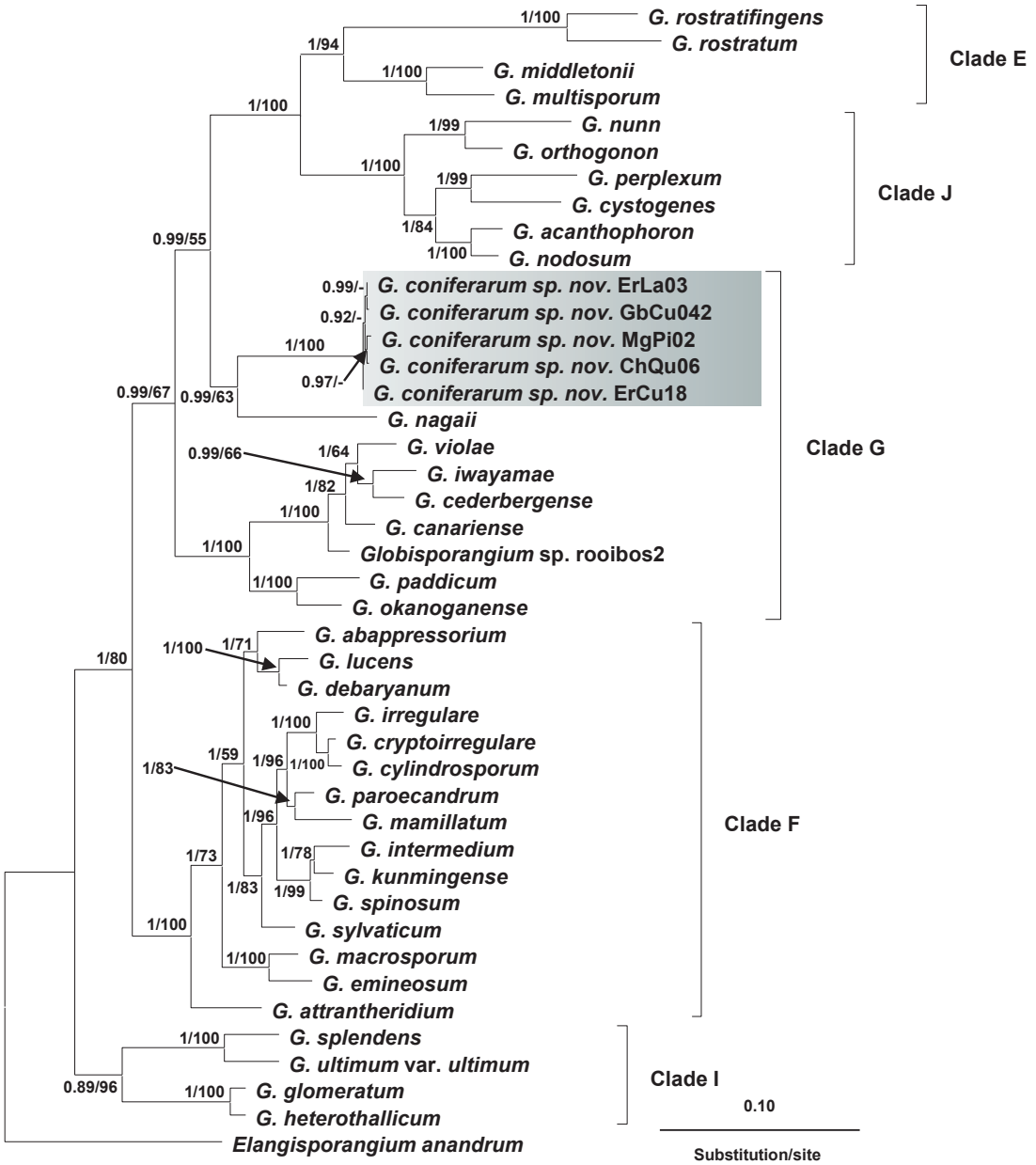

Fig. 1. Phylogenetic relationships of *Globisporangium* isolates from conifers and *Quercus* sp. (Shiraz County, Iran) among 20 *Globisporangium* species based on Bayesian analysis of multigene genealogies of nuclear (ITS and *β*tub) and mitochondrial (*cox1* and *cox2*) sequences. Numbers on branches represent posterior probability based on Bayesian analysis and the bootstrap support based on maximum likelihood analysis, respectively.

Notes: *Globisporangium coniferarum* belongs to clade 4 of *Globisporangium sensu* Uzuhashi *et al.* (2010), clustering in the proximity of *G. nagaii* (Fig. 1). *Globisporangium coniferarum* is differentiated from other known species by its high temperature requirement, amorphous oogonia, its specific vesicle formation and zoospore release, and its unique sequences of mitochondrial and nuclear genes. Isolates were recovered from various sites in Shiraz County in Iran.

DISCUSSION

During 2013–2019, diverse oomycete isolates including 500 *Pythium sensu lato* isolates were sourced from rhizosphere soil of ornamental trees in Shiraz County. The great number and diversity of *Pythium* species (Salmaninezhad & Mostowfizadeh-Ghalamfarsa 2019a) recovered during the survey indicate that high humidity and warm temperatures in urban gardens provide a favourable ecological niche for these soilborne microorganisms. The majority of *Pythium s.l.* isolates recovered from ornamental trees were referred to the genus *Globisporangium sensu* Uzuhashi *et al.* (2010). Phylogenetic analysis revealed a new distinct lineage in *Globisporangium* encompassing isolates with peculiar morphological traits which differentiate this group of isolates from all other described *Globisporangium* species. This lineage was formally described as a new species, *G. coniferarum*, an epithet stressing that most of these isolates were recovered from conifers. The split of *Pythium* into five distinct genera and the segregation of *Globisporangium* as a separate genus by Uzuhashi *et al.* (2010) were questioned by De Cock *et al.* (2015) as this, although justified based on morphological characters and nomenclaturally valid, was not well-supported by phylogenetic analysis. Consequently, authors in general have been cautious in using the name *Globisporangium* to describe

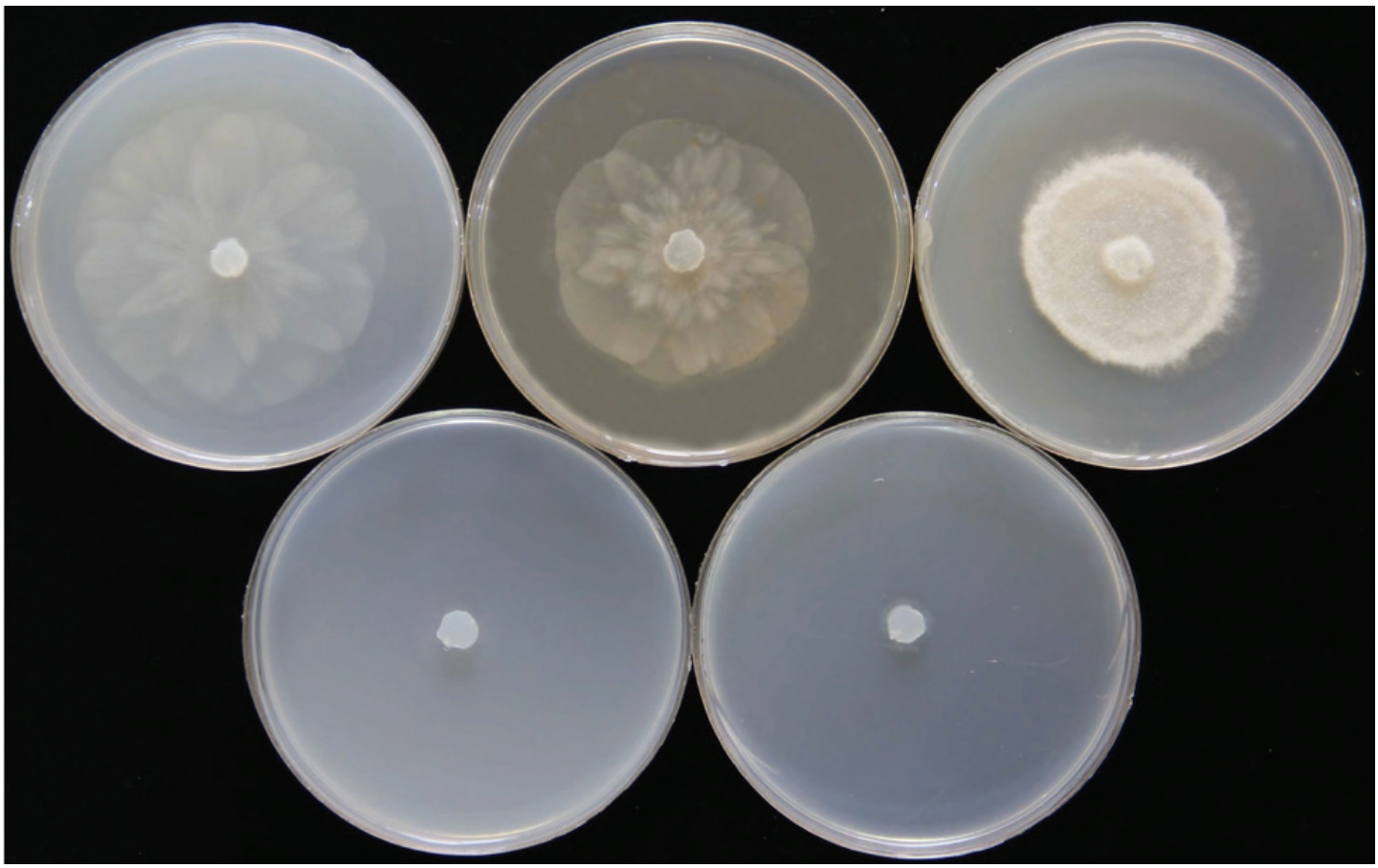

Fig. 2. Colony morphology of *Globisporangium coniferarum* CBS 148568 (after 48 h) on various media at 25 °C; top (from left to right): carrot agar, malt extract agar and potato-dextrose agar; bottom (from left to right): cornmeal agar and hempseed agar.

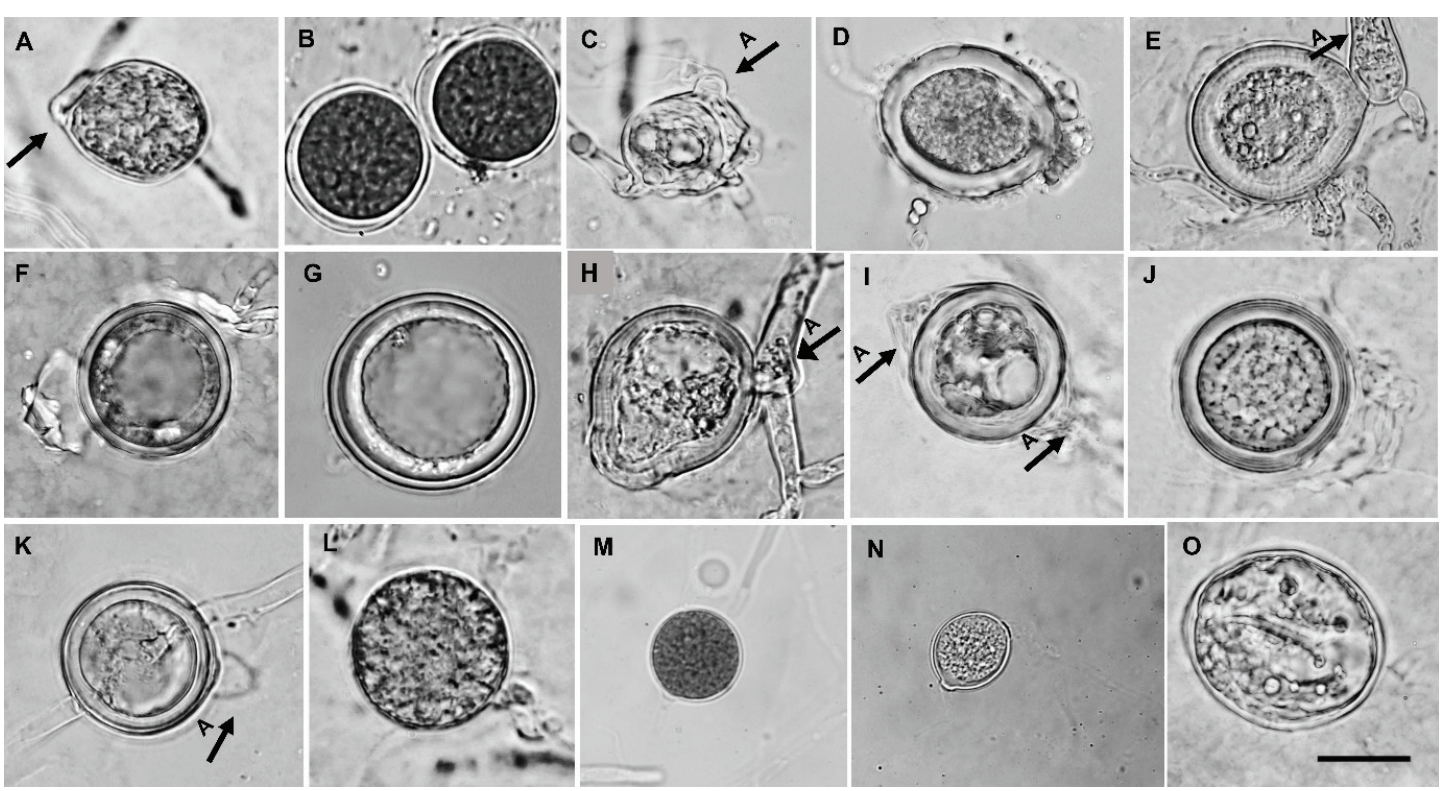

Fig. 3. Morphology of *Globisporangium coniferarum*. **A, B.** Sporangia: **A.** Terminal ovoid sporangium with pedicel (arrow); **B.** Globose sporangia. **C–K.** Sexual structures: **C.** Formation of intercalary aplerotic oogonium with paragynous diclinous antheridium (arrow); **D.** Plerotic ellipsoid oospore; **E.** Asymmetrical plerotic oospore with diclinous clavate antheridium (arrow); **F.** Plerotic terminal oospore; **G.** Nearly aplerotic globose oospore; **H.** Ovoid oospore with intercalary, paragynous and diclinous antheridium (arrow); **I.** Intercalary plerotic oospore with hypogynous antheridia (arrows); **J.** Globose oospore; **K.** Intercalary nearly aplerotic oospore with paragynous, monoclinous antheridium originated near oogonium (arrow). **L–N.** Chlamydospores: **L.** Terminal globose chlamydospore; **M.** Intercalary globose chlamydospore; **N.** Intercalary ovoid chlamydospore. **O.** Amorphous to ovoid chlamydospore. Scale bar = 10 µm.

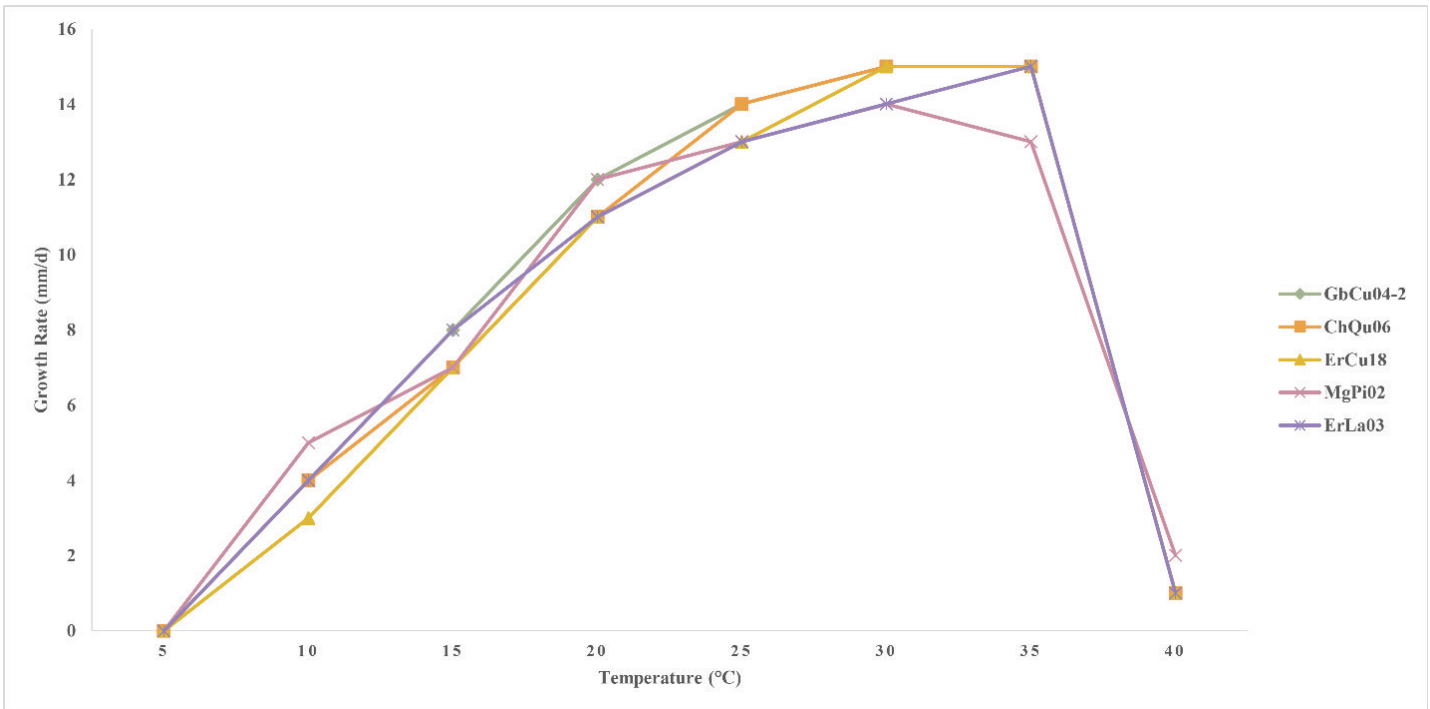

Fig. 4. Average radial growth rate of *Globisporangium coniferarum* isolates on potato-dextrose agar at different temperatures.

new species or report new records, and in most cases they have preferred the well-established name *Pythium*. Despite this, after the formal introduction of the genus *Globisporangium*, there have been numerous reports of *Globisporangium* species from across the world and a few have been from Iran (Bolboli & Mostowfizadeh-Ghalamfarsa 2015, Salmaninezhad & Mostowfizadeh-Ghalamfarsa 2017, 2019a). Quite recently, a new species, *G. lacustre*, has been described formally and two new nomenclatural combinations were added to the genus (Uzuhashi *et al.* 2019). In the taxonomic revision of Nguyen *et al.* (2022) not only the distinction between *Globisporangium* and *Pythium s.s.* has been corroborated by phylogenomic analysis, but also the use of the name *Globisporangium sensu* Uzuhashi *et al.* (2010) has been recommended.

Phylogenetically, *Globisporangium coniferarum* is closely related to *G. nagaii, G. violae, G. cederbergense, G. okanoganense, G. paddicum, G. iwayamae,* and *G. canariense.* Furthermore, according to the *cox1* phylogeny (Fig. S2), *G. coniferarum* appeared as a sister taxon to *G. monoclinum,* which was not consistent with the ITS tree where *G. monoclinum* was a diverged lineage to clade G of *Globisporangium*. Several unique morphological features separate *G. coniferarum* from other species. For instance, *G. nagaii* is known to produce sporangia with proliferation whereas no proliferation has been observed in *G. coniferarum* isolates. Moreover, *G. nagaii* has been reported to produce monoclinous and single antheridia, smooth and terminal oogonia (Van der Plaats-Niterink 1981), while *G. coniferarum* produces irregular oogonia and monoclinous or diclinous, clavate antheridia. Besides, cardinal temperatures for *G. nagaii* are 9, 28 and 35 °C, while cardinal temperatures for *G. coniferarum* are higher, *i.e.*, 15, 30 and 40 °C, respectively.

Sporangial production is unknown in *G. violae*. It only forms aplerotic oospores with up to eight sessile-shaped antheridia which are mostly monoclinous (Van der Plaats-Niterink 1981). Unlike abundant zoospore production in *G. coniferarum*, *G. violae* has never been reported to produce zoospores. Symmetrical oospores and paragynous antheridia were rarely observed in *G. coniferarum,* whereas *G. violae* is known to produce only symmetrical oospores with mostly monoclinous antheridia. Besides, *G. violae* produces aerial mycelium on CMA (Van der Plaats-Niterink 1981), while no aerial mycelium was observed on any media in case of *G. coniferarum.* Moreover, cardinal temperatures for *G. violae* isolates were between 5 and 35 °C (Van der Plaats-Niterink 1981), while in *G. coniferarum* were between 15 to 40 °C and the isolates could not tolerate less than 9 °C.

Globisporangium cederbergense does not produce zoospores (Bahramisharif *et al.* 2013). However, production of terminal and globose hyphal swellings, terminal, or intercalary oospores with up to two monoclinous antheridia has been reported in this species (Bahramisharif *et al.* 2013). Furthermore, terminal to intercalary hyphal swellings, clavate antheridia, and both mono- and diclinous antheridia were observed in *G. coniferarum*. Additionally, *G. cederbergense* is known to produce only aplerotic oospores (Bahramisharif *et al.* 2013), whereas *G. coniferarum* produces both plerotic and aplerotic oospores. Minimum temperature for growth in *G. cederbergense* is 3 to 5 °C, whereas *G. coniferarum* could not tolerate temperatures below 15 °C.

Globisporangium okanoganense produces only terminal sporangia with different shapes, *i.e.*, from globose to pyriform which are infrequently proliferating and borne in sympodial succession (Van der Plaats-Niterink 1981) whereas *G. coniferarum* does not have proliferated sporangia and sympodial succession was never observed in this species. Although both *G. coniferarum* and *G. okanoganense* produce smooth, terminal to intercalary oospores with monoclinous to diclinous antheridia, *G. okanoganense* is well-known to have globose to subglobose oogonia with unequally thickness in its wall and antheridia are terminally attached to the oogonium (Van der Plaats-Niterink 1981). However, *G. coniferarum* produces mostly asymmetrical oogonia with both terminal and lateral attached antheridia to

oogonia. Besides, antheridial stalks are mostly swollen in *G. okanoganense* which was not observed in *G. coniferarum.*

Formation of ornamented oospores with up to four antheridia separates *G. paddicum* from *G. coniferarum* (Van der Plaats-Niterink 1981). None of the isolates assigned to *G. coniferarum* evaluated in this study produced ornamented oogonia.

The most closely related species to *G. coniferarum* is *G. iwayamae* regarding its morphology. They both produce terminal to intercalary, smooth oogonia, mono- or diclinous, clavate antheridia, globose chlamydospores, and ovoid to ellipsoid sporangia (Van der Plaats-Niterink 1981). However, production of both terminal and intercalary sporangia, mostly plerotic oospores, more antheridia per oogonium (up to 5) and unbranched antheridial stalks by *G. coniferarum,* completely separates it morphologically from *G. iwayamae.* Besides, cardinal temperatures in *G. iwayamae* are 5, 25, and 30 °C, while in *G. coniferarum* are 15, 30, and 40 °C.

Globisporangium canariense forms spherical to pyriform papillate, intercalary, and sometimes catenulate sporangia with up to six antheridia per oogonium which crowded the oogonium (Paul 2002). However, *G. coniferarum* does not have any catenulated sporangia and no more than five antheridia were observed in this species. Besides, apical and lateral attachment of antheridia to oogonia, production of pedicellate sporangia, and specific formation of zoospores in *G. coniferarum* separates it from *G. canariense.*

Globisporangium monoclinum does not produce any sporangia or zoospores which separates it from *G. coniferarum* (Badali *et al.* 2020). In addition, catenulated oogonia was reported in *G. monoclinum* (Badali *et al.* 2020), which was never observed in *G. coniferarum*. *Globisporangium monoclinum* has only been identified based on ITS and *cox1* loci, hence, we did not add it to our concatenated phylogeny.

Production of abundant chlamydospores in liquid media is a unique characteristic of *G. coniferarum,* which separates it from all other known *Globisporangium* species. Moreover, formation of pedicellate sporangia, slow release of zoospores, amorphous oogonia, clavate, paragynous to hypogynous antheridia differentiated this species from other known *Globisporangium* species.

Multiple gene genealogy studies of nuclear (ITS and *βtub*) and mitochondrial (*cox2* and *cox1*) sequences revealed that all isolates examined in this study formed a monophyletic group in clade G of *Pythium sensu* Lévesque & de Cock (2004) which is now included in *Globisporangium* (Uzuhashi *et al.* 2010, Nguyen *et al.* 2022). Analysing the ITS region of the clones showed that the maximum nucleotide diversity can be observed in ITS1 and ITS2 regions. Aligning these sequences with other *Globisporangium* species sequences showed that all *Globisporangium* species show this diversity in their ITS1 and ITS2 regions (Table S4). Hence, it can be concluded that all *Globisporangium* species have very conserved yet diverse ITS1 and ITS2 regions, similar to other *Pythium s.l.* species which separates them as a different genus.

The presence of multiple divergent copies of the ITS region is a well-known character among *Pythium s.l.* species, such as *Phytopythium helicoides*, *Pp. litorale, Pp. mercuriale, Pp. vexans* complex*, G. mamillatum, G. splendens, G. heterothallicum, G. rostratifingenes*, *G. irregulare, G. cryptoirregulare*, *G. ultimum, G. spinosum, G. perplexum, P. acanthicum* complex, *P. arrhenomanes* and *P. graminicola* (Kageyama *et al.* 2007, Belbahri *et al.* 2008, McLeod *et al.* 2009, Spies *et al.* 2011). All the mentioned species have intraspecific ITS sequence variability. *Globisporangium coniferarum* ITS sequences of the clones showed that the ITS region of *G. coniferarum* had many insertions (data not shown). These insertions led to the overlapping of the direct sequences, disruption of the electropherograms, and consequently low-quality sequences. Furthermore, *G. coniferarum* isolates also showed intraspecific ITS sequence variability (Table S2). In addition, sequences had multiple tandem repeats (data not shown). Using the resulting contigs of ITS clones, we showed that *G. coniferarum* is a new species located in a separate lineage close to *G. nagaii.* Other loci sequences (*i.e.*, *βtub, cox1,* and *cox2*) showed a very high quality and strongly supported the separation of this new species.

Members of clade E, F, G, and I of *Pythium s.l.* are known to produce ovoid and internally proliferating sporangia as well as oogonia with smooth walls (Uzuhashi *et al.* 2016). The exception is *P. paddicum* which produces ornamented oospores. The results showed that *G. coniferarum* isolates had these features and are closely related to *G. nagaii, G. nunn, G. perplexum,* and *G. rostratum.* However, morphological and phylogenetic analyses strongly discriminate *G. coniferarum* as a new taxon. Data of *βtub* sequences did not show any signs of ambiguous signals in nucleotide positions that could be inferred as evidence for hybrid origin of this lineage. Phylogenetic analysis of ITS regions derived from cloning-based sequencing also revealed the same results and showed that *G. coniferarum* is a new species close to *G. nagaii*.

This study describes a new *Globisporangium* species in clade G of *Pythium s.l.* found prevalently associated with the roots and rhizosphere soil of conifers and recovered occasionally also from rhizosphere soil of *Quercus* sp. in Iran. The ecology, pathogenicity and the host-range of this new species deserve to be further investigated to clarify its role, if any, in the decline of ornamental trees in urban gardens of Iran.

ACKNOWLEDGEMENTS

Authors would like to thank Prof. Marco Thines for his valuable technical assistance. They wish to thank Mrs Ann Davis for revising the English text. This research was funded by the Iran National Science Foundation (INSF, award number 4001002) and by the University of Catania, Italy, Investigation of phytopathological problems of the main Sicilian productive contexts and eco-sustainable defense strategies (MEDIT-ECO) PiaCeRi-PIAno di inCEntivi per la Ricerca di Ateneo 2020-22 linea 2 5A722192155. F.A. has been granted a fellowship by the PON RICERCA E INNOVAZIONE 2014–2020, Azione II – Obiettivo Specifico 1b – Progetto Miglioramento delle produzioni agroalimentari mediterranee in condizioni di carenza di risorse idriche – WATER4AGRIFOOD, cod. CUP: B64I20000160005.

Conflict of interest: The authors declare that there is no conflict of interest.

REFERENCES

Altschul SFW, Gish W, Miller EW, *et al.* (1990). Basic local alignment search tool. *Journal of Molecular Biology* **215**: 403–410.

Bahramisharif A, Lamprecht SC, Spies CF, *et al.* (2013). *Pythium cederbergense sp. nov*. and related taxa from *Pythium* clade G associated with the South African indigenous plant *Aspalathus*

linearis (rooibos). *Mycologia* **105**: 1174–1189.

Badali F, Abrinbana M, Abdollahzadeh J (2020). Morphological and molecular taxonomy of *Pythium monoclinum* Abrinbana, Abdollahz. & Badali, *sp. nov*., and *P. iranense sp. nov.,* from Iran. *Cryptogamie Mycologie* **41**: 179–191.

Barber PA, Paap T, Burgess TI, *et al.* (2013). A diverse range of *Phytophthora* species are associated with dying urban trees. *Urban Forestry & Urban Greening* **12**: 569–575.

Belbahri L, McLeod A, Paul B, *et al.* (2008). Intraspecific and within-isolate sequence variation in the ITS rRNA gene region of *Pythium mercuriale sp. nov.* (*Pythiaceae*). *FEMS Microbiology Letters* **284**: 17–27.

Bolboli Z, Mostowfizadeh-Ghalamfarsa R (2015). Phylogenetic relationships and taxonomic characteristics of *Pythium* spp. isolates in cereal fields of Fars province. *Iranian Journal of Plant Pathology* **51**: 471–492.

Bonants P, Hagenaar-de Weerdt M, *et al.* (1997). Detection and identification of *Phytophthora fragariae* Hickman by polymerase chain reaction. *European Journal of Plant Pathology* **103**: 345–355.

Cooke DEL, Drenth A, Duncan JM, *et al.* (2000). A molecular phylogeny of *Phytophthora* and related oomycetes. *Fungal Genetics and Biology* **30**:13–32.

Darvas JM, Scott DB, Kotze JM (1978). Fungi associated with damping-off in coniferous seedlings in South African nurseries. *South African Forestry Journal* **104**: 15–19.

De Cock AWAM, Lodhi AM, Rintoul TL, *et al.* (2015). *Phytopythium*: molecular phylogeny and systematics. *Persoonia* **34**: 25–39.

Elvira-Recuenco M, Cacciola SO, Sanz-Ros AV *et al.* (2020). Potential interactions between invasive *Fusarium circinatum* and other pine pathogens in Europe. *Forests* **11**: 7.

Ershad D (2009). *Fungi of Iran.* 2nd edn. Iranian Research Institute of Plant Protection: Tehran, Iran.

Erwin DC, Ribeiro O (1996). *Phytophthora diseases worldwide.* 1st edn. APS Press: St Paul, MN, USA.

Felsenstein J (1993). *PHYLIP (phylogeny inference package)*. Version 3.5c. Distributed by the author, Seattle, USA: University of Washington, Department of Genetics.

Giordana G, Kitzberger T, La Manna L (2020). Anthropogenic factors control the distribution of a southern conifer Phytophthora disease in a peri-urban area in northern Patagonia, Argentina. *Forests* **11**: 1183.

Hall TA (1999). BioEdit: a user-friendly biological sequence alignment editor and analysis program for Windows 95/98/NT. *Nucleic Acid Science* **41**: 95–98.

Ho HH, Chen XX, Zeng HC, *et al.* (2012). The occurrence distribution of *Pythium* species in Hanian South Island of China. *Botanical Studies* **53**: 525–534.

Jeffers SN, Martin SB (1968). Comparison of two media selective for *Phytophthora* and *Pythium* species. *Plant Disease* **70**: 1035–1043.

Jung T, La Spada F, Pane A *et al.* (2019). Diversity and distribution of *Phytophthora* species in protected natural areas in Sicily. *Forests* **10**: 259.

Kageyama K, Senda M, Asano T, *et al.* (2007). Intra-isolate heterogeneity of the ITS region of rDNA in *Pythium helicoides*. *Mycological Research* **111**: 416–423.

Khdiar MY, Barber PA, Hardy GEStJ, *et al.* (2020). Association of *Phytophthora* with declining vegetation in an urban forest environment. *Microorganisms* **8**: 973–989.

Kobayashi S, Uzuhashi S, Tojo M, *et al.* (2010). Characterization of *Pythium nunn* newly recorded in Japan and its antagonistic activity against *P. ultimum* var. *ultimum. Journal of General Plant Pathology* **76**: 278–283.

La Spada F, Cock PJA, Randall E *et al.* (2022). DNA metabarcoding and isolation by baiting complement each other in revealing *Phytophthora* diversity in anthropized and natural ecosystems. *Journal of Fungi* **8**: 330.

Lazreg F, Belabid L, Sanchez J, *et al.* (2013). First report of *Globisporangium ultimum* causing Pythium Damping-Off on Aleppo Pine in Algeria, Africa, and the Mediterranean Region. *Plant Disease* **97**: 1111.

Lévesque CA, De Cock AW (2004). Molecular phylogeny and taxonomy of the genus *Pythium*. *Mycological Research* **108**: 1363–1383.

McLeod A, Botha WJ, Meitz JC, *et al.* (2009). Morphological and phylogenetic analysis of *Pythium* species in South Africa. *Mycological Research* **113**: 933–951.

Mirabolfathy M, Ershad D (1993). Isolation of *Phytophthora* species from root, crown and stem of ornamental plants. *Iranian Journal of Plant Pathology* **29**: 62–70.

Mirabolfathy M, Ershad D (1996). Studies on the conifer damping-off in the forest nurseries of northern and central Iran. *Iranian Journal of Plant Pathology* **32**: 6–13.

Mirsoleimani Z, Mostowfizadeh-Ghalamfarsa R (2013). Characterization of *Phytophthora pistaciae*, the causal agent of pistachio gummosis, based on host range, morphology and ribosomal genome. *Phytopathologia Mediterranea* **53**: 501–506.

Moncalvo JM, Wang HH, Hseu RS (1995). Phylogenetic relationships in *Ganoderma* inferred from the internal transcribed spacers and 25S ribosomal DNA sequences. *Mycologia* **87**: 223–223.

Mostowfizadeh-Ghalamfarsa R (2016). *Pythium species in Iran*. 1st edn. Shiraz University Press, Shiraz, Iran.

Mostowfizadeh-Ghalamfarsa R, Banihashemi Z (2005). Identification of soil *Pythium* species in Fars Province of Iran. *Iranian Journal of Science and Technology Transaction A-Science* **29**: 79–87.

Mostowfizadeh-Ghalamfarsa R, Cooke DEL, Banihashemi Z (2008). *Phytophthora parsiana sp. nov*., a new high-temperature tolerant species. *Mycological Research* **112**: 783–794.

Nowak DJ, Walton JT (2005). Projected urban growth (2000–2050) and its estimated impact on the US forest resource. *Journal of Forest* **103**: 383–389.

Nylander JAA (2004). MrModeltest v. 2.3. Program distributed by the author. Sweden: Uppsala University, Evolutionary Biology Centre.

Nguyen HDT, Dodge A, Dadej K *et al.* (2022). Whole genome sequencing and phylogenomic analysis show support for the splitting of genus *Pythium*. *Mycologia* **114**: 501–515.

Paul B (2002). ITS region of *Pythium canariense sp. nov.*, its morphology and its interaction with *Botrytis cinerea*. *FEMS Microbiology Letters* **208**: 135–141.

Riolo M, Aloi F, La Spada F, *et al.* (2020). Diversity of *Phytophthora* communities across different type of Mediterranean vegetation in a nature reserve area. *Forests* **11**: 853–874.

Robideau GP, De Cock AWAM, Coffey MD, *et al.* (2011). DNA barcoding of oomycetes with cytochrome c oxidase subunit I and internal transcribed spacer. *Molecular Ecology Resources* **11**: 1002–1011.

Rounquist F, Huelsenbeck JP (2003). MrBayes 3: Bayesian phylogenetic inference under mixed models. *Bioinformatics* **19**: 1572–1574.

Safaeifarahani B, Mostowfizadeh-Ghalamfarsa R, Hardy GEStJ, *et al.* (2015). Re-evaluation of *Phytophthora cryptogea* species complex and the description of a new species, *Phytophthora pseudocryptogea sp. nov*. *Mycological Progress* **14**: 108–120.

Salmaninezhad F, Mostowfizadeh-Ghalamfarsa R (2017). Taxonomy, phylogeny and pathogenicity of *Pythium* species in rice paddy fields of Fars Province. *Iranian Journal of Plant Pathology* **53**: 31–53.

Salmaninezhad F, Mostowfizadeh-Ghalamfarsa R (2019a). Oomyceteous flora of ornamental trees of Shiraz County (Iran). *Rostaniha* **20**: 29–43.

Salmaninezhad F, Mostowfizadeh-Ghalamfarsa R (2019b). Three new *Pythium* species from rice paddy fields. *Mycologia* **111**: 274–290.

Schmitthenner AF (1973). Isolation and identification methods for *Phytophthora* and *Pythium*. Proceedings of the Woody Ornamental Disease Workshop. Colombia, Missouri, USA, 24th Jan. 1973, University of Missouri: 128.

Spies CFJ, Mazzola M, McLeod A (2011). Characterization and detection of *Pythium* and *Phytophthora* species associated with grapevines in South Africa. *European Journal of Plant Pathology* **131**: 103–119.

Stöver BC, Müller KF (2010). TreeGraph 2: combining and visualizing evidence from different phylogenetic analyses. *BMC Bioinformatics* **11**: 1–9.

Swofford D (2002). *PAUP*: Phylogenetic analysis using parsimony (*and other methods)*. Sunderland: Sinauer Associates.

Tan KH (1996). *Soil sampling, preparation and analysis*. 1st edn. Marcel Dekker Inc. New York, USA.

Thompson JD, Gibson TJ, Plewniak F, *et al.* (1997). The ClustalX windows interface: flexible strategies for multiple sequence alignment aided by quality analysis tools. *Nucleic Acids Research* **25**: 4876–4882.

Uzuhashi S, Hata K, Matsuura S, *et al.* (2016). *Globisporangium oryzicola sp. nov*., causing poor seedling establishment of directly seeded rice. *Antonie van Leeuwenhoek* **110**: 543–552.

Uzuhashi S, Ikeda H, Kamekawa A, *et al.* (2019). Presence of two species-level groups in *Globisporangium splendens* isolates in Japan. *European Journal of Plant Pathology* **154**: 751–766.

Uzuhashi S, Nakagawa S, Abdelzaher HMA, *et al.* (2019). Phylogeny and morphology of new species of *Globisporangium*. *Fungal Systematics and Evolution* **3**: 13–18.

Uzuhashi S, Tojo M, Kakishima M (2010). Phylogeny of the genus *Pythium* and description of new genera. *Mycoscience* **51**: 337–365.

Van der Plaats-Niterink AJ (1981). Monograph of the genus *Pythium. Studies in Mycology* **21**: 1–244.

Villa NO, Kageyama K, Asano T, *et al.* (2006). Phylogenetic relationships of *Pythium* and *Phytophthora* species based on ITS rDNA, cytochrome oxidase II and β-tubulin gene sequences. *Mycologia* **98**: 410–422.

White TJ, Bruns T, Lee S, Taylor JW (1990). Amplification and direct sequencing of fungal ribosomal RNA genes for phylogenetics, In: *PCR protocols: a guide to methods and applications.* (Innis MA, Gelfand DH, Sninsky JJ, White TJ, eds). Academic Press, USA: 315–322.

Supplementary Material: http://fuse-journal.org/

Fig. S1. Phylogenetic relationships of *Globisporangium* spp. from conifers and *Quercus* sp. (Shiraz County, Iran) among 17 *Globisporangium* species based on Bayesian analysis of *ϐtub* sequences. Numbers on branches represent posterior probability based on Bayesian analysis and the bootstrap support based on maximum likelihood analysis, respectively.

Fig. S2. Phylogenetic relationships of *Globisporangium* spp. from conifers and *Quercus* sp. (Shiraz County, Iran) among 16 *Globisporangium* species based on Bayesian analysis of *cox1* sequences. Numbers on branches represent posterior probability based on Bayesian analysis and the bootstrap support based on maximum likelihood analysis, respectively.

Fig. S3. Phylogenetic relationships of *Globisporangium* spp. from conifers and *Quercus* sp. (Shiraz County, Iran) among 17 *Globisporangium* species based on Bayesian analysis of *cox2* sequences. Numbers on branches represent posterior probability based on Bayesian analysis and the bootstrap support based on maximum likelihood analysis, respectively.

Fig. S4. Phylogenetic relationships of *Globisporangium* spp. from conifers and *Quercus* sp. (Shiraz County, Iran) among 33 *Globisporangium* species based on Bayesian analysis of Internal transcribed spacer (ITS) sequences. Numbers on branches represent posterior probability based on Bayesian analysis and the bootstrap support based on maximum likelihood analysis, respectively.

Table S1. List of primers used in this study.

Table S2. Polymerase chain reaction conditions for primers used in this study.

Table S3. Information of all the *Globisporangium* isolates used in the phylogenetic analyses, including local, international, and alternative isolate identifications. GenBank accession numbers for sequences obtained in present study are shown in bold.

Table S4. Base pairs differences across *ϐ-tub,* ITS, *cox1* and *cox2* sequences showing the inter- and intraspecific variation of *G. coniferarum* (CON), and other related species, including, *G. nagaii* (NAG), *G. violae* (VIO), *G. paddicum* (PAD), *G. okanoganense* (OKA), *G. canariense* (CAN), *G. monoclinum* (MON), and *G. iwayamae* (IWA).